Strong correlation between ionic bonding strength and superconductivity in compressed hydrides

Xing Li [1,*], Zixuan Guo,[1,*] Yansun Yao [2,†] Xiaohua Zhang [1] Shicong Ding,[1] and Guochun Yang [1,3,‡]

[1]*State Key Laboratory of Metastable Materials Science & Technology and Key Laboratory for Microstructural Material Physics of Hebei Province, School of Science, Yanshan University, Qinhuangdao 066004, China*

[2]*Department of Physics and Engineering Physics, University of Saskatchewan, Saskatoon, Saskatchewan, Canada S7N 5E2*

[3]*Centre for Advanced Optoelectronic Functional Materials Research and Key Laboratory for UV Light-Emitting Materials and Technology of Northeast Normal University, Changchun 130024, China*

Understanding the superconductivity in relation to chemical bonding is essential for the development of superconductors. We propose that pressure-reduced ionic bonding strength is beneficial for improving superconductivity in hydrides (negative correlation between bonding strength and critical temperature). We model ionic hydrides using a prototypical ionic lattice (CsCl-type) with simple-valence metal Li/Rb and hydrogen and control the bonding strength via external pressure. First-principles calculations reveal that the ionic bonding strength in LiH increases with pressure while its critical temperature (T_c) simultaneously decreases. A higher T_c at lower pressures is attributed to stronger electron-phonon coupling (EPC) induced by weaker ionic bonds and significant EPC contributions from mid-frequency phonons. RbH's pressure dependences of bonding strength and T_c are the reverse of those of LiH, and the EPC primarily results from high-frequency phonons. The distinct interorbital electron transition mechanism and amounts of charge transfer are responsible for the opposite trend of changes in bonding strength and superconductivity in LiH and RbH. The proposed correlation is further validated by the other six ionic hydrides. Substantial T_c change (e.g., 126.2 K at 100 GPa and 5.7 K at 300 GPa in LiH) in response to bonding strength variation reveals a key factor for designing new superconductors.

I. INTRODUCTION

One of the most challenging quests in condensed matter physics is the preparation of room-temperature superconductors [1–3]. Conventional superconductors' critical temperatures (T_c) are associated with the effective coupling between electrons and phonons. Chemical bonds, which directly reflect the structural properties of a compound, can influence electron-phonon coupling (EPC) [4,5]. Covalent bond, in particular, has shown the ability to manipulate the superconductivity [4–8]. Boron-doped diamond exhibits superconductivity due to an unsaturated σ bond induced by electron-deficient boron [4,9,10]. Tuning the antibonding occupancy can stabilize the weakly bonded hydrogen cages, i.e., an intermediate between hydrogen's molecular and metallic phases, which is the prototypic structure of high-T_c clathrate hydrides [11–14]. Moreover, it has been shown that increasing the unsaturation of covalent bonds or weakening their bonding strengths can enhance the T_c in P-rich sulfides, MH$_9$ (M = Y, Th, and Pr), and H$_3$S doped with Si, C, and P atoms [6].

Other than stabilizing the crystal structure, ionic bonds can directly contribute to the superconductivity [15,16]. Yet, previous studies on superconducting hydrides have primarily focused on the chemical precompression of hydrogen species by metal atoms [11,17–19]; the actual effects of M-H (M = metal atoms) bonds on the superconductivity should be given more attention [20]. Various superconducting properties in clathrate Y/La/CeH$_{10}$ [19,21,22] and Ca/YH$_6$ [23,24], having the same hydrogen cage, are associated with different ionic bonds in these compounds. Moreover, the pressure dependence of superconductivity in ionic hydrides is nonmonotonic, i.e., the T_c of AlH$_3$/ScH$_3$ decreases/increases with pressure [25,26]. In this context, elucidating ionic bonds and their role in superconductivity is essential for designing superconductors, particularly metal hydrides.

In this work, we employ a typical ionic model, the CsCl-type structure, and study the influence of ionic bonds on hydride superconductivity. Two elements from group I, Li and Rb, are chosen to construct simple hydrides LiH and RbH. Despite both being near-free electron metals, Li and Rb have distinct valence properties under high pressure induced by interorbital electron transfers [27,28], making them contrasting case studies for bonding formation. The strength of the Li-H and Rb-H bonds can be controlled by external pressure. Moreover, it is interesting to note that alkali metals can act a bit like hydrogen once sufficiently compressed; Li, especially, can form diatomic-molecule-like structures under high pressure [29]. Hydrogen, conversely, can behave like alkali metals under high pressure, adopting nonmolecular structures and becoming metallic [30]. It is therefore interesting to investigate the intertwined bonding between alkali metals and hydrogen and its implication for superconductivity. Despite Li and Rb having distinct valence configurations [27,28] and reversed

---

*These authors contributed equally to this work.

†Contact author: yansun.yao@usask.ca

‡Contact author: yanggc468@nenu.edu.cn
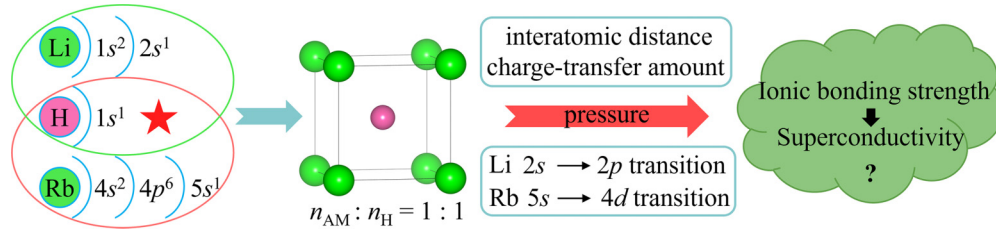
FIG. 1. Design principle, crystal structure, and strategy to regulate the bonding strength in ionic hydrides. The high-symmetry CsCl-type structure composed of Li/Rb and H atoms is selected as a model, and external pressure is used to control the bonding strength and valence configuration of Li and Rb.

electronegativity [31] at high pressures, LiH and RbH follow the same trend for superconductivity: weakening ionic bonding strength is conducive to improving T_c. Our results make a significant step toward understanding the role of ionic bonding strength in superconductivity.

II. METHOD

The crystal structures were visualized using the VESTA software [32]. Structural relaxations and electronic properties were calculated with the Vienna *ab initio* Simulation Package (VASP) [33]. The projector augmented wave (PAW) method [34,35] was adopted with $1s^2 2s^1/4s^2 4p^6 5s^1$ and $1s^1$ valence states for Li/Rb and H atoms, respectively, with Perdew-Burke-Ernzerhof (PBE) functional [36]. To ensure energy convergence, a planewave cutoff energy of 950 eV and Monkhorst-Pack grids with $2\pi \times 0.03$ Å^{-1} density were employed. The Bader charge analysis was used to determine the charge transfer [37], and the electron localization function (ELF) was used to characterize chemical bonds [38]. Phonon calculations were performed using the supercell finite displacement method in the PHONOPY code [39]. EPC calculations were conducted within the density functional perturbation theory (DFPT) in the QUANTUM ESPRESSO package [40].

III. RESULTS

A. Research model

To study the effects of ionic bonds on superconductivity, we model the prototypical ionic structures (NaCl- and CsCl-type) with Li/Rb and H atoms (Fig. 1). The significant difference in electronegativity induces ionic bonding between alkali metals and hydrogen, while the external pressure controls the bonding strength. The calculated thermodynamic stability shows that the enthalpy of the CsCl-type phase is lower than that of the NaCl-type phase for RbH in the pressure range of 8–271 GPa (Fig. S1, Supplemental Material [41]; see also [42–44]), while the enthalpy reversal above 271 GPa suggests the possible existence of other low-enthalpy phases. For LiH, the enthalpy of the CsCl-type phase is consistently higher from 0 to 300 GPa, while their enthalpy difference gradually decreases with pressure. These results are similar to previous studies [45,46]. Notably, CsCl-type LiH and RbH exhibit a wide pressure range of dynamic stability and good metallicity (100–300 and 200–300 GPa, respectively), providing an excellent platform for exploring the superconductivity associated with ionic bonds (Figs. S2, S3, S4). Accordingly, the CsCl-type phase is the focus of our discussion (Fig. 1).

B. Structural and electronic properties

For the LiH phase at 100 GPa (Fig. 1), each atom is coordinated with eight atoms of the opposite type with a bond length of 1.67 Å. The ionicity of the Li-H bond is characterized by the amount of charge transfer between Li and H atoms [Fig. 2(a)] and the electron distribution in the ELF plot [Fig. S5(a)]. The nearest H-H distance is 1.93 Å, much longer than 0.74 Å in molecule hydrogen [47], which would exclude the formation of covalent bonds in the crystal. Therefore, LiH
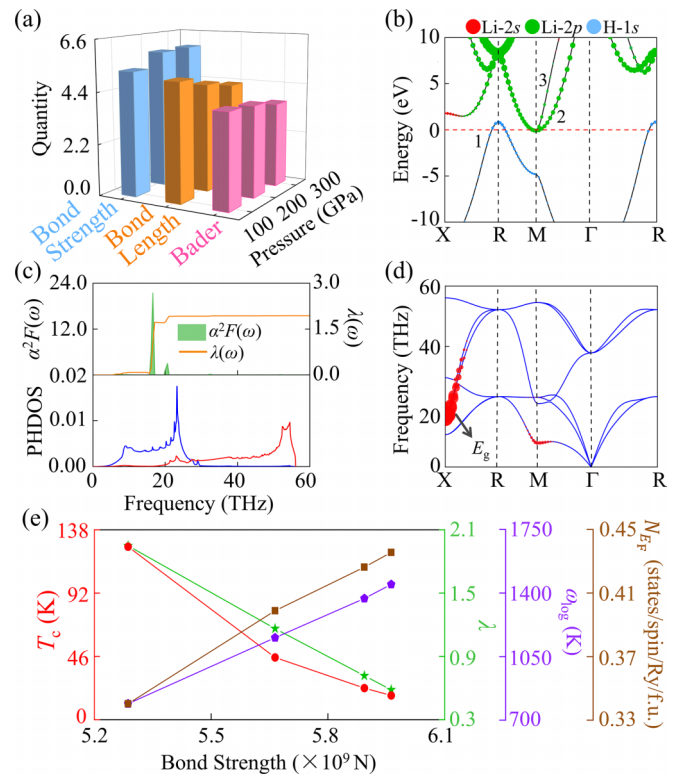
FIG. 2. (a) Pressure-dependent charge transfer (e$^-$), Li-H bond length (Å) and strength (N) of the CsCl-type LiH phase. For clarity, the values of transferred charge and Li-H bond length are magnified 3 and 5 times, while the value of Li-H bond strength is reduced 10^9 times and taken as an absolute value. (b) Electronic band structure where the bands crossing the E_F are numbered. (c) Eliashberg spectral function $\alpha^2F(\omega)$, EPC parameter $\lambda(\omega)$, phonon density of states (PHDOS), and (d) phonon dispersion curves (thickness of the red dots indicates the modes' contribution to λ) of the CsCl-type LiH phase at 100 GPa. (e) The T_c, λ, ω_{log}, and N_{E_F} associated with the Li-H bonding strength.
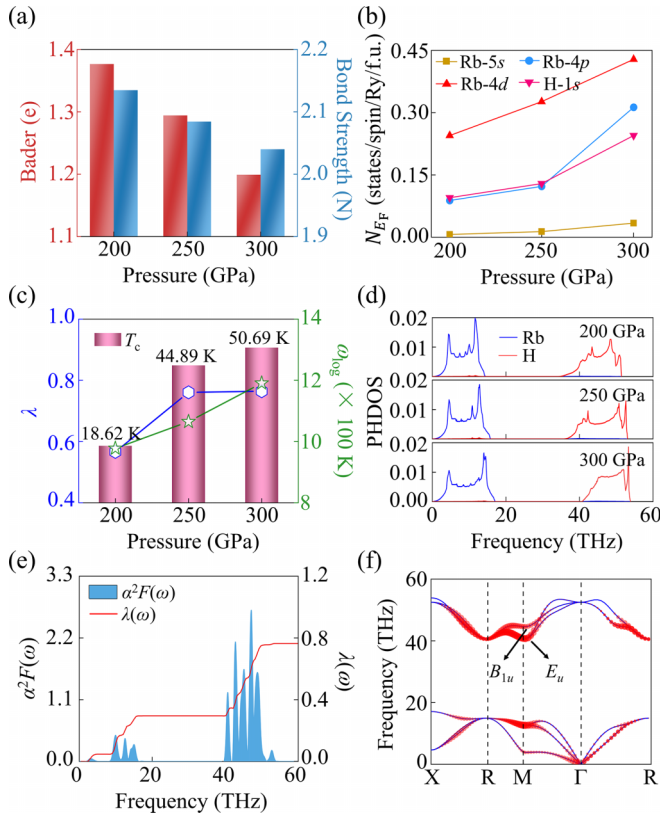
FIG. 3. (a) Pressure-dependent charge transfer and strength of Rb-H ionic bond in the CsCl-type RbH phase. For clarity, the bond strength is reduced by 10^9 times and is taken as an absolute value. (b) Orbital projected N_{E_F}, (c) T_c, λ, $\omega_{\log}$, and (d) PHDOS of the RbH under pressure. (e) $\alpha^2 F(\omega)$, $\lambda(\omega)$, and (f) phonon dispersion curves (thickness of the red dots indicates the modes' contribution to λ) at 300 GPa.

is a purely ionic compound, and the same applies to RbH [Fig. S5(b)].

Based on the electronic density of states (DOS) and band structures, LiH and RbH are metallic at pressures above 100 and 200 GPa, respectively (Figs. S3, S4). The closure of the band gap in LiH is due to the pressure-induced overlap of H $1s$ bands (electrons) and the Li $2p$ bands (holes) [Fig. 2(b)]. For RbH, the DOS at the Fermi level is primarily from Rb $4d$ states and a small amount of Rb $4p$ and H $1s$ states [Fig. 3(b)]. This observation is consistent with the pressure-induced Li $2s \rightarrow 2p$ and Rb $5s \rightarrow 4d$ interorbital electron transitions [27,28]. The metallicity of LiH and RbH are confirmed using HSE06 hybrid functional calculations (Fig. S6). In the following, we investigate the correlation between ionic bonding strength and the LiH superconductivity, then extend it to RbH for comparison and to broaden the findings.

C. Correlation between ionic bonding strength and superconductivity

The strength of an ionic bond is associated with the Coulomb interaction between cation and anion. At high pressures, the transferred charge and the distance between Li and H concurrently decrease where the influence of distance

change is more significant, resulting in an overall increased Li-H Coulomb interaction based on the Coulomb's law $F = k_e q_1 q_2 / r^2$ [Fig. 2(a)]. On the other hand, the charge-transfer amount from Li to H is negatively correlated with the DOS at the Fermi level [N_{E_F}, Fig. 2(e)], whereas the Li-H ionic bonding strength is positively correlated.

By employing the Migdal-Eliashberg theory [48], we estimate the T_c of LiH and RbH, and establish the relation between superconductivity and ionic bonding strength. The LiH phase exhibits a phonon-mediated superconductivity from 100 to 300 GPa (Table S2), and its pressure-dependent T_c value is inversely proportional to the Li-H ionic bonding strength [Fig. 2(e) and Table S2], demonstrating an obvious negative correlation character. Moreover, its T_c value varies from 126.2 K at 100 GPa to 5.7 K at 300 GPa, reflecting a visible influence of ionic bonds on the superconductivity. On the other hand, the variation of T_c is consistent with the EPC constant (λ), but opposite to the logarithmic average phonon frequency ($\omega_{\log}$) and N_{E_F}. This clearly indicates that λ dominates the evolution of T_c.

The larger λ at lower pressures in LiH can be attributed to the reduced Fermi velocity and significant phonon softening near the X point [Figs. 2(b), 2(d) and S7]; the latter is evidenced by the substantial contribution to λ by this mode (Fig. S8). In detail, the contribution of mid-frequency phonon vibrations to the total λ is up to 95% at 100 GPa, similar to the case of TeH$_4$ with Te-H ionic bonds [49]. From 100 to 300 GPa, these softened phonons are associated with the E_g mode, mainly contributed by the H atoms (Fig. S9), but the degree of softening gradually decreases due to the pressure-induced bond strengthening. Furthermore, at 100 GPa, the Fermi velocity associated with band 2 is as low as 0.9 [Fig. S7(b)], originating from the small electron pocket almost tangent to the E_F around the M point [Fig. 2(b)]. At 300 GPa, the upward shift of the E_F contributes to a larger electron pocket and steeper slope of the band 2 near the E_F, resulting in a noticeable increase in the Fermi velocity [Fig. S7(e)]. In general, low Fermi velocity facilitates a strong EPC [50,51] through a stronger Fermi surface nesting, and therefore, the increased Fermi velocity at higher pressure leads to a decreased λ. The increasing $\omega_{\log}$ at high pressure results from a higher average phonon frequency induced by the stronger Li-H ionic bond (Table S2), which is unfavorable for the improvement of λ, according to its definition formula $\lambda = 2 \int d\omega \frac{\alpha^2 F(\omega)}{\omega}$ [44].

It is well known that λ, $\omega_{\log}$, N_{E_F}, and Fermi velocity are four key parameters that determine superconductivity. For our case, these parameters are all correlated with the ionic bonding strength. As ionic bond becomes stronger, the degree of phonon softening decreases and the Fermi velocity enhances, which in turn reduces λ, while both $\omega_{\log}$ and N_{E_F} progressively increase. Thus, the strength of ionic bonding indirectly influences the superconductivity.

Interestingly, the amount of charge transfer in RbH significantly reduces at high pressures, resulting in a weaker Rb-H bond [Fig. 3(a)]. The primary cause for this trend, which is opposite to that in LiH, is the pressure-induced s-d electron transition in Rb and the reversal of electronegativity order between Li and Rb [28,31]. In this case, the N_{E_F} in RbH primarily comes from the contribution of Rb $4d$ electrons [Fig. 3(b)]. For the superconductivity of RbH, its T_c is

positively correlated with λ, $\omega_{\log}$, and N_{E_F}, which all increase with pressure [Figs. 3(b), 3(c)]. Noteworthily, the vibrational modes of Rb and H atoms in RbH are essentially separated [Fig. 3(d)]. This is due to the significant difference in atomic mass, as well as the weak Rb-H ionic bond caused by the large discrepancy in electronegativity and interatomic distance. Although the degree of phonon softening is more significant at lower pressures, the high-frequency vibrations of hydrogen (B_{1u} and E_u modes, Fig. S12) make a dominating contribution to the total λ at high pressures (Figs. S10, S11), which along with a significantly increased N_{E_F} [especially for Rb 4d electrons, Fig. 3(b)], resulting in a high T_c. This mechanism differs from the increased λ induced by the enhanced phonon softening and the reduced Fermi velocity in LiH.

However, the pressure-induced variations of N_{E_F} and $\omega_{\log}$ in RbH are consistent with the LiH phase [Figs. 3(b) and 3(c)]. Consequently, the difference in pressure-dependent superconducting mechanisms between LiH and RbH is mainly reflected in the discrepant origin of the EPC, owing to the distinct Li/Rb atomic attribute. Interestingly, despite this, they both agree that reduced ionic bonding strength is beneficial for high T_c.

To further examine the effect of ionic bonds on superconductivity and to better compare with LiH/RbH, we select the previously reported ionic hydrides with the same stoichiometry, where one metal contains d-electrons while the other does not, such as AlH$_3$ without d-electrons and ScH$_3$ with d-electrons [25,26]. Interestingly, AlH$_3$/ScH$_3$ show the same T_c vs ionic bonding strength trends under pressure as LiH/RbH (Table S4). Moreover, the established relation between ionic bonding strength and superconductivity also holds for some other ionic hydrides of HfH$_2$ [52], VH$_3$ [53], GaH$_3$ [16], and CaH$_4$ [54] (Table S5). Thus, as mentioned above, the metal atoms in ionic hydrides indeed have certain effects on the pressure dependence of superconductivity, which is mainly reflected in their ionic bonding strength.

D. Superconducting mechanism

Based on the above analysis, we explore T_c and the origin of superconductivity in LiH at 100 GPa and RbH at 300 GPa. For LiH, the calculated λ is 1.94, which is slightly lower than 2.19 for H$_3$S at 200 GPa and 2.29 for LaH$_{10}$ at 250 GPa [19,55], indicating that the ionic bond also favors the strong EPC. Based on the contributions of N_{E_F} and phonons to λ mentioned above, it can be concluded that the coupling between the H-derived mid-frequency phonons and the Li 2p and H 1s electrons dictates its superconductivity. Considering its strong EPC, the Allen-Dynes modified McMillan equation containing two separate correction factors (f_1 and f_2) is utilized to estimate the T_c of LiH [44]. The estimated T_c value is 126.4 K at 100 GPa, assuming a typical Coulomb pseudopotential $\mu^* = 0.10$ [56,57], which is in close proximity to that of many superhydrides, e.g., 116 K for KH$_{12}$ at 150 GPa and 126.2 K for TiH$_{22}$ at 350 GPa [58,59]. For RbH, the estimated λ and T_c values at 300 GPa are 0.76 and 50.77 K (Table S3), respectively. These values are lower than those of LiH at 100 GPa, as a result of the lower N_{E_F} and

increased phonon frequency induced by the different chemical attributes of the Li and Rb atoms. Its superconductivity predominantly originates from the interaction between H-derived high-frequency phonons and Rb 4d electrons.

IV. CONCLUSION

In summary, we have used an ionic model (CsCl-type) for LiH and RbH to study the superconductivity and its correlation with the ionic bonding strength. In both compounds, weaker ionic bond favors superconductivity, which occurs at low pressures in LiH and high pressures in RbH. As a result, the T_cs in these two compounds vary differently with the pressure. In LiH, the low Fermi velocity and the enhanced phonon softening induced by the weakened Li-H bond result in higher T_cs at lower pressures. As for RbH, a higher T_c at higher pressures is attributed to the simultaneous increase of λ and $\omega_{\log}$, originating from the increased N_{E_F} associated with the weakened Rb-H ionic bond and the elevated average phonon frequency. To be noted, our unveiled relation also applies to other ionic hydrides. On the other hand, we have revealed that the s-p electron transition of a metal atom induces a weak bonding strength at lower pressures, whereas the s-d electron transition favors weak bonding strength at higher pressures, which can guide the metal atom selection in the design of pressure-dependent superconductors. Our established correlation is consistent with that we have previously proposed in covalent systems [6], where weakening covalent bonding strength promotes the enhancement of critical temperature. Finally, for hydrides containing both ionic and covalent bonds, external conditions such as pressure can cause varying degrees of change in these bonding strengths, resulting from competition, mutual facilitation, or inhibition between the two kinds of bonds. The complexity of these interactions is beyond the scope of the current model, but needs to be urgently addressed in future research, which might offer some important hints for the design of hydride superconductors.

[1] A. P. Drozdov, M. I. Eremets, I. A. Troyan, V. Ksenofontov, and S. I. Shylin, Conventional superconductivity at 203 kelvin at high pressures in the sulfur hydride system, Nature (London) **525**, 73 (2015).

[2] A. P. Drozdov, P. P. Kong, V. S. Minkov, S. P. Besedin, M. A. Kuzovnikov, S. Mozaffari, L. Balicas, F. F. Balakirev, D. E. Graf, V. B. Prakapenka *et al.*, Superconductivity at 250 K in lanthanum hydride under high pressures, Nature (London) **569**, 528 (2019).

[3] J. A. Flores-Livas, L. Boeri, A. Sanna, G. Profeta, R. Arita, and M. Eremets, A perspective on conventional high-temperature superconductors at high pressure: Methods and materials, Phys. Rep. **856**, 1 (2020).

[4] E. Bustarret, J. Kačmarčik, C. Marcenat, E. Gheeraert, C. Cytermann, J. Marcus, and T. Klein, Dependence of the superconducting transition temperature on the doping level in single-crystalline diamond films, Phys. Rev. Lett. **93**, 237005 (2004).

[5] B. Liu, W. Cui, J. Shi, L. Zhu, J. Chen, S. Lin, R. Su, J. Ma, K. Yang, M. Xu, Effect of covalent bonding on the superconducting critical temperature of the H-S-Se system, Phys. Rev. B **98**, 174101 (2018).

[6] X. Li, X. Zhang, Y. Liu, and G. Yang, Bonding-unsaturation-dependent superconductivity in P-rich sulfides, Matter Radiat. Extremes **7**, 048402 (2022).

[7] Y. Ge, F. Zhang, and Y. Yao, First-principles demonstration of superconductivity at 280 K in hydrogen sulfide with low phosphorus substitution, Phys. Rev. B **93**, 224513 (2016).

[8] Y. Sun, X. Li, T. Iitaka, H. Liu, and Y. Xie, Crystal structures and superconductivity of carbonaceous sulfur hydrides at pressures up to 300 GPa, Phys. Rev. B **105**, 134501 (2022).

[9] X. Blase, C. Adessi, and D. Connétable, Role of the dopant in the superconductivity of diamond, Phys. Rev. Lett. **93**, 237004 (2004).

[10] M. Calandra and F. Mauri, High-T_c superconductivity in superhard diamondlike BC$_5$, Phys. Rev. Lett. **101**, 016401 (2008).

[11] Y. Sun, J. Lv, Y. Xie, H. Liu, and Y. Ma, Route to a superconducting phase above room temperature in electron-doped hydride compounds under high pressure, Phys. Rev. Lett. **123**, 097001 (2019).

[12] J. Bi, Y. Nakamoto, P. Zhang, K. Shimizu, B. Zou, H. Liu, M. Zhou, G. Liu, H. Wang, and Y. Ma, Giant enhancement of superconducting critical temperature in substitutional alloy (La,Ce)H$_9$, Nat. Commun. **13**, 5952 (2022).

[13] W. Chen, X. Huang, D. V. Semenok, S. Chen, D. Zhou, K. Zhang, A. R. Oganov, and T. Cui, Enhancement of superconducting properties in the La-Ce-H system at moderate pressures, Nat. Commun. **14**, 2660 (2023).

[14] W. Zhao, D. Duan, M. Du, X. Yao, Z. Huo, Q. Jiang, and T. Cui, Pressure-induced high-T_c superconductivity in the ternary clathrate system Y-Ca-H, Phys. Rev. B **106**, 014521 (2022).

[15] Q. Zhuang, X. Jin, T. Cui, Y. Ma, Q. Lv, Y. Li, H. Zhang, X. Meng, and K. Bao, Pressure-stabilized superconductive ionic tantalum hydrides, Inorg. Chem. **56**, 3901 (2017).

[16] G. Gao, H. Wang, A. Bergara, Y. Li, G. Liu, and Y. Ma, Metallic and superconducting gallane under high pressure, Phys. Rev. B **84**, 064118 (2011).

[17] X. Liang, A. Bergara, L. Wang, B. Wen, Z. Zhao, X.-F. Zhou, J. He, G. Gao, and Y. Tian, Potential high-T_c superconductivity in CaYH$_{12}$ under pressure, Phys. Rev. B **99**, 100505(R) (2019).

[18] X.-L. He, P. Zhang, Y. Ma, H. Li, X. Zhong, Y. Wang, H. Liu, and Y. Ma, Potential high-temperature superconductivity in the substitutional alloy of YSrH$_{11}$ under high pressure, Phys. Rev. B **107**, 134509 (2023).

[19] H. Liu, I. I. Naumov, R. Hoffmann, N. W. Ashcroft, and R. J. Hemley, Potential high-T_c superconducting lanthanum and yttrium hydrides at high pressure, Proc. Natl. Acad. Sci. **114**, 6990 (2017).

[20] W. E. Pickett, Colloquium: Room temperature superconductivity: The roles of theory and materials design, Rev. Mod. Phys. **95**, 021001 (2023).

[21] F. Peng, Y. Sun, C. J. Pickard, R. J. Needs, Q. Wu, and Y. Ma, Hydrogen clathrate structures in rare earth hydrides at high pressures: Possible route to room-temperature superconductivity, Phys. Rev. Lett. **119**, 107001 (2017).

[22] B. Li, Z. Miao, L. Ti, S. Liu, J. Chen, Z. Shi, and E. Gregoryanz, Predicted high-temperature superconductivity in cerium hydrides at high pressures, J. Appl. Phys. **126**, 235901 (2019).

[23] H. Wang, J. S. Tse, K. Tanaka, T. Iitaka, and Y. Ma, Superconductive sodalite-like clathrate calcium hydride at high pressures, Proc. Natl. Acad. Sci. USA **109**, 6463 (2012).

[24] Y. Li, J. Hao, H. Liu, J. S. Tse, Y. Wang, and Y. Ma, Pressure-stabilized superconductive yttrium hydrides, Sci. Rep. **5**, 9948 (2015).

[25] M. Shao, S. Chen, W. Chen, K. Zhang, X. Huang, and T. Cui, Superconducting ScH$_3$ and LuH$_3$ at megabar pressures, Inorg. Chem. **60**, 15330 (2021).

[26] Y.-K. Wei, N.-N. Ge, X.-R. Chen, G.-F. Ji, L.-C. Cai, and Z.-W. Gu, *Ab initio* studies on phase transition, thermoelastic, superconducting and thermodynamic properties of the compressed cubic phase of AlH$_3$, J. Appl. Phys. **115**, 124904 (2014).

[27] B. Rousseau, Y. Xie, Y. Ma, and A. Bergara, Exotic high pressure behavior of light alkali metals, lithium and sodium, Eur. Phys. J. B **81**, 1 (2011).

[28] A. K. McMahan, Alkali-metal structures above the *s-d* transition, Phys. Rev. B **29**, 5982 (1984).

[29] J. B. Neaton and N. W. Ashcroft, Pairing in dense lithium, Nature (London) **400**, 141 (1999).

[30] J. M. McMahon and D. M. Ceperley, High-temperature superconductivity in atomic metallic hydrogen, Phys. Rev. B **84**, 144515 (2011).

[31] M. Rahm, R. Cammi, N. W. Ashcroft, and R. Hoffmann, Squeezing all elements in the periodic table: Electron configuration and electronegativity of the atoms under compression, J. Am. Chem. Soc. **141**, 10253 (2019).

[32] K. Momma and F. Izumi, VESTA3 for three-dimensional visualization of crystal, volumetric and morphology data, J. Appl. Cryst. **44**, 1272 (2011).

[33] J. Hafner, *Ab-initio* simulations of materials using VASP: Density-functional theory and beyond, J. Comput. Chem. **29**, 2044 (2008).

[34] G. Kresse and J. Furthmüller, Efficient iterative schemes for *ab initio* total-energy calculations using a plane-wave basis set, Phys. Rev. B **54**, 11169 (1996).

[35] P. E. Blöchl, Projector augmented-wave method, Phys. Rev. B **50**, 17953 (1994).

[36] J. P. Perdew, J. A. Chevary, S. H. Vosko, K. A. Jackson, M. R. Pederson, D. J. Singh, and C. Fiolhais, Atoms, molecules, solids, and surfaces: Applications of the generalized gradient

approximation for exchange and correlation, Phys. Rev. B **46**, 6671 (1992).

[37] W. Tang, E. Sanville, and G. Henkelman, A grid-based Bader analysis algorithm without lattice bias, J. Phys.: Condens. Matter **21**, 084204 (2009).

[38] A. D. Becke and K. E. Edgecombe, A simple measure of electron localization in atomic and molecular systems, J. Chem. Phys. **92**, 5397 (1990).

[39] S. Baroni, S. de Gironcoli, A. Dal Corso, and P. Giannozzi, Phonons and related crystal properties from density-functional perturbation theory, Rev. Mod. Phys. **73**, 515 (2001).

[40] P. Giannozzi, S. Baroni, N. Bonini, M. Calandra, R. Car, C. Cavazzoni, D. Ceresoli, G. L. Chiarotti, M. Cococcioni, and I. Dabo, QUANTUM ESPRESSO: A modular and open-source software project for quantum simulations of materials, J. Phys: Condens. Matter **21**, 395502 (2009).

[41] See Supplemental Material at http://link.aps.org/supplemental/10.1103/PhysRevMaterials.8.084805 for computational details; structural information, phonon dispersion curves, electronic band structures, PDOS, ELF, and superconducting properties of CsCl-type LiH and RbH; correlation between ionic bonding strength and T_c of six other ionic hydrides.

[42] J. P. Carbotte, Properties of boson-exchange superconductors, Rev. Mod. Phys. **62**, 1027 (1990).

[43] P. B. Allen and B. Mitrović, Theory of superconducting T_c, Solid State Phys. **37**, 1 (1983).

[44] P. B. Allen and R. C. Dynes, Transition temperature of strong-coupled superconductors reanalyzed, Phys. Rev. B **12**, 905 (1975).

[45] S. Biswas, I. Errea, M. Calandra, F. Mauri, and S. Scandolo, *Ab initio* study of the LiH phase diagram at extreme pressures and temperatures, Phys. Rev. B **99**, 024108 (2019).

[46] I. O. Bashkin, E. G. Ponyatovskii, and Y. M. Dergachev, Pressure-induced phase transition in RbH, Phys. Stat. Sol. **130**, 73 (1985).

[47] E. Wigner and H. B. Huntington, On the possibility of a metallic modification of hydrogen, J. Chem. Phys. **3**, 764 (1935).

[48] J. Bardeen, L. N. Cooper, and J. R. Schrieffer, Theory of superconductivity, Phys. Rev. **108**, 1175 (1957).

[49] X. Zhong, H. Wang, J. Zhang, H. Liu, S. Zhang, H.-F. Song, G. Yang, L. Zhang, and Y. Ma, Tellurium hydrides at high pressures: High-temperature superconductors, Phys. Rev. Lett. **116**, 057002 (2016).

[50] X. Zhang, M. Zhao, and F. Liu, Enhancing superconductivity in bulk β-Bi_2Pd by negative pressure induced by quantum electronic stress, Phys. Rev. B **100**, 104527 (2019).

[51] J. M. An and W. E. Pickett, Superconductivity of MgB_2: Covalent bonds driven metallic, Phys. Rev. Lett. **86**, 4366 (2001).

[52] Y. Liu, X. Huang, D. Duan, F. Tian, H. Liu, D. Li, Z. Zhao, X. Sha, H. Yu, H. Zhang *et al.*, First-principles study on the structural and electronic properties of metallic HfH_2 under pressure, Sci. Rep. **5**, 11381 (2015).

[53] Q. Zhuang, X. Jin, Q. Lv, Y. Li, Z. Shao, Z. Liu, X. Li, H. Zhang, X. Meng, K. Bao and T. Cui, Investigation of superconductivity in compressed vanadium hydrides, Phys. Chem. Chem. Phys. **19**, 26280 (2017).

[54] Z. Shao, D. Duan, Y. Ma, H. Yu, H. Song, H. Xie, D. Li, F. Tian, B. Liu, and T. Cui, Unique phase diagram and superconductivity of calcium hydrides at high pressures, Inorg. Chem. **58**, 2558 (2019).

[55] D. Duan, Y. Liu, F. Tian, D. Li, X. Huang, Z. Zhao, H. Yu, B. Liu, W. Tian, and T. Cui, Pressure-induced metallization of dense $(H_2S)_2H_2$ with high-T_c superconductivity, Sci. Rep. **4**, 6968 (2014).

[56] P. Morel and P. W. Anderson, Calculation of the superconducting state parameters with retarded electron-phonon interaction, Phys. Rev. **125**, 1263 (1962).

[57] A. Sanna, J. A. Flores-Livas, A. Davydov, G. Profeta, K. Dewhurst, S. Sharma, and E. K. U. Gross, *Ab initio* Eliashberg theory: Making genuine predictions of superconducting features, J. Phys. Soc. Jpn. **87**, 041012 (2018).

[58] D. V. Semenok, I. A. Kruglov, I. A. Savkin, A. G. Kvashnin, and A. R. Oganov, On distribution of superconductivity in metal hydrides, Curr. Opin. Solid State Mater. Sci. **24**, 100808 (2020).

[59] J. Zhang, J. M. McMahon, A. R. Oganov, X. Li, X. Dong, H. Dong, and S. Wang, High-temperature superconductivity in the Ti-H system at high pressures, Phys. Rev. B **101**, 134108 (2020).